Temperature-controlled neutron reflectometry sample cell suitable for study of photoactive thin films

Kevin G. Yager,[a] Oleh M. Tanchak,[b] and Christopher J. Barrett[c]
Department of Chemistry, McGill University, Lab 406, 801 Sherbrooke Street W., Montreal, Quebec H3A 2K6, Canada

Mike J. Watson[d] and Helmut Fritzsche[e]
Chalk River Laboratories, Building 459, Station 18, Chalk River, Ontario K0J 1J0, Canada

We describe a novel cell design intended for the study of photoactive materials using neutron reflectometry. The cell can maintain sample temperature and control of ambient atmospheric environment. Critically, the cell is built with an optical port, enabling light irradiation or light probing of the sample, simultaneous with neutron reflectivity measurements. The ability to measure neutron reflectivity with simultaneous temperature ramping and/or light illumination presents unique opportunities for measuring photoactive materials. To validate the cell design, we present preliminary results measuring the photoexpansion of thin films of azobenzene polymer. © *2006 American Institute of Physics.* [DOI: 10.1063/1.2194090]

INTRODUCTION

Neutron reflectometry is a powerful technique for studying thin films of any composition, including organic thin films, and biological samples. The technique is based upon the detection of grazing-angle specularly reflected neutrons. At very low angles, a neutron beam will be totally reflected by a sample-ambient interface. With increase in the specular reflection angle, oscillations in the reflection amplitude can be seen. These so-called Kiessig fringes[1] are characteristic of the sample's structure, most notably the thickness and neutron refractive index. The neutron refractive index is related to the scattering length density (SLD) of the material's constituent atoms. Consistent with conventional Fresnel theory, interfaces between differing refractive indices (or, in the case of neutrons, differing SLDs) will lead to reflection. The reflectivity as a function of angle is generally expressed in terms of the momentum transfer, or scattering vector,

$$q_z = \frac{4\pi}{\lambda} \sin \theta,$$

where λ is the wavelength of the incident neutron beam, and θ is the specular scattering angle. The exact shape of the neutron reflectivity curve is a function of the film structure in the normal direction. From this, one can deduce film thickness, density, and roughness. With more elaborate model fitting, one can also deduce multilayer structures or internal material gradients. The technique is applicable to films in the thickness range of about 10–2000 Å. Neutrons, unlike x rays, are sensitive to light elements (such as H, C, N, O),

making them more suitable for studying polymers, biological samples, and other soft matter. Additionally, because the scattering length varies with isotope, one can enhance the neutron reflectivity signal by making isotopic substitutions, which often have no effect on chemistry or material properties. One can also perform difference experiments, where two samples that differ only in the isotopic nature of one of their constituent atoms are compared to determine the spatial distribution of that atom. More details on the technique of neutron reflectometry can be found elsewhere.[2]

Neutron reflectometry has additional unique advantages when applied to studying photoactive materials. There is currently considerable interest in thin films that respond to, control, or otherwise interact with light in the ultraviolet (UV), visible and infrared (IR) bands of the electromagnetic spectrum. Such materials find application in telecommunications (as routers, couplers, filters, etc.), in the microelectronics industry (as photoresists), as photoactuators, photonic band gap materials, and so on.[3] Such materials often cannot be studied using optical techniques, because their interaction with light would confuse the measurement, or, in many cases, the photoprobe would be modifying the sample during measurement. For instance, materials used for photoresists may undergo photopolymerization or photodegradation. Azobenzene materials, which will be described later in more detail, are known to isomerize under illumination, and to photoalign when irradiated with polarized light.[4] Even using nominally nonabsorbing wavelengths, some measure of photoalignment, hence birefringence, may be induced.[5] This time-varying birefringence makes conventional optical techniques, such as ellipsometry, more difficult to apply to photoactive materials. Similarly, photonic band gap materials have unique interactions with light that make conventional optical techniques (such as ellipsometry, optical reflectivity, surface plasmon resonance, etc.) difficult to interpret. In some cases, nonperturbing optical measurements are not pos-

[a]FAX: +1 (514) 398-2382; electronic mail: kevin.yager@mail.mcgill.ca
[b]FAX: +1 (514) 398-2382; electronic mail: oleh.tanchak@mail.mcgill.ca
[c]FAX: +1 (514) 398-3797; electronic mail: christopher.barrett@mcgill.ca
[d]FAX: +1 (613) 584-4040; electronic mail: mike.watson@nrc.gc.ca
[e]FAX: +1 (613) 584-4040; electronic mail: helmut.fritzsche@nrc.gc.ca

77, 045106-1

sible, whereas in other cases, complimentary measurements to confirm optical characterization would be valuable. It is thus of interest to investigate nonoptical measurement techniques that can be used on photoactive materials. Ideally, the techniques would allow for light illumination during measurement, which would enable one to measure photochanges in real time, and without otherwise perturbing the sample. X-ray reflectometry is capable of resolving the structure of a thin film in the normal direction with high accuracy, and could be coupled with simultaneous light illumination. However, since the scattering intensity of x rays increases with total electron density, hence atomic number, it is a technique best suited to inorganic and metallic thin films. The scattering intensity of neutrons, by contrast, is determined by nuclear properties, and can be very high for lighter elements, including H, C, N, and O. Also, x rays may lead to material damage for some samples, whereas the lower energy of thermal neutrons minimizes material damage. Thus, neutron reflectivity is, in some cases, better suited to the study of organic and biological samples, compared to x-ray reflectivity. In particular, a great number of photofunctional materials (including resists and photonic band gap structures) are based on organic polymers. In other cases, the differing scattering properties of a material to x rays and neutrons can be used for comparative experiments, where ambiguities can be resolved. Overall, neutron reflectivity offers the possibility to study photoactive samples in a nondestructive and unambiguous way, determining any changes in thickness and density due to irradiation.

Given that neutron reflectometry is nearly universally applicable to thin films, experiment design becomes limited only by the availability of appropriate sample environments during scanning. It is thus of interest to explore novel sample cells that can enable measurement of neutron reflectivity at the same time that sample illumination is performed. Simultaneous control of the sample's ambient environment (temperature, humidity, etc.) is also useful.[6] Here we report on a new sample chamber that was designed to enable neutron reflectivity experiments to be carried out on photoactive materials, without the need to remove the sample from the neutron beam in order to irradiate it. The sample cell additionally enables control of temperature and ambient atmosphere. This sample setup is validated with preliminary experiments measuring nonthermal photoexpansion effects when azobenzene-polymer thin films are irradiated with laser light. Although this sample cell has been conceived of for reflectometry of thin films, it could easily be adapted to other neutron scattering techniques (SANS, diffraction, etc.), where the sample can be irradiated with visible laser light without removing it from the neutron beam.

CONSTRUCTION AND PERFORMANCE DETAILS

The internal design of the cell is shown in Fig. 1 (the cell enclosure can be seen in Fig. 4). The sample is attached to a large copper plate, centered inside an aluminum enclosure. The aluminum sidewalls allow the neutron beam to pass through with very little attenuation. The front port is equipped with a window, allowing for illumination of the
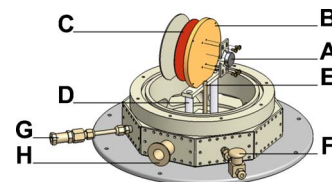

FIG. 1. (Color online) Exploded view of the sample disk and environmental control features. The silicon substrate (A) is attached to the copper block (B) with restraints positioned above and below. The block is maintained at the correct temperature by a heating element (C) bonded to the back of the plate. The sample and block are thermally isolated by insulating ceramic posts (D) and can be quenched to lower temperature by flowing gas out of the quench tube (E). The base of the cell can be equipped with a variety of attachments, allowing for supply of quench gas (inlet F and effluent G), evacuation of the cell (vacuum flange H).

sample at normal or near-normal incidence. The window can be made of polymethyl methacrylate (PMMA, also known as Plexiglas or Lucite), glass, quartz, or other materials as determined by optical requirements. The cell lid and front window rest on rubber O rings, which form a tight seal when the cell is evacuated. These two pieces can also be screwed securely, enabling the cell to be used with a positive pressure with respect to ambient. The base of the cell is equipped with ports for controlling the cell's atmosphere.

The sample is a silicon wafer, 24 mm in diameter and 6 mm thick, coated with the thin film under investigation. The wafer is secured against a large copper plate using fasteners above and below the sample (A in Fig. 1). Thermoconductive paste was used to provide a good thermal conduction between the sample and copper plate. In principle, larger sample sizes could be accommodated in this cell, although the small sample size is advantageous in optical studies (as described later). The back of the copper block has a 125 W resistive heating element clamped to it (C in Fig. 1). A temperature sensor reads the temperature of the copper block, and a feedback loop ensures that the sample is held at the proper temperature. Measurements were made of the temperature differential between the heating block and the sample by bonding a thermocouple directly on the surface of a Si wafer. It was found that the deviation of the sample temperature from the block temperature increases with increasing temperature, e.g., 2 K deviation at 383 and 4 K deviations at 453 K. The sample/heating setup is held in place with two Macor® insulating glass-ceramic posts (D in Fig. 1). This thermally isolates the sample and the sample heater from the rest of the cell. The cell environment can be modified using the ports built into the base of the enclosure (F, G, and H in Fig. 1). Ports allow for evacuation of the cell using a vacuum pump, purging with ambient atmosphere, or the introduction of an arbitrary atmosphere from other equipment (such as gas cylinders). In particular, the quench port exits directly onto the sample, making ideal for quickly cooling samples down to room temperature using a cool stream of an inert gas.

The cell was specifically designed to enable temperature ramping of the sample. This allows for neutron measurements at a variety of sample temperatures, which can be useful in, for instance, the identification of phase transitions in materials, or the determining of activation energies. For
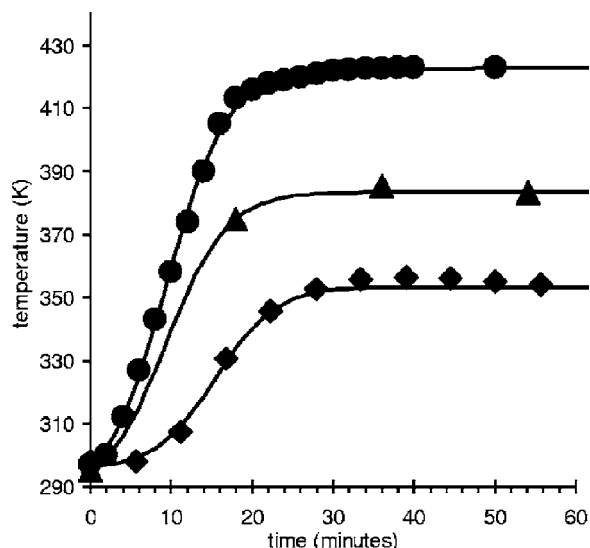
FIG. 2. Typical temperature ramping behavior of the sealed sample cell. The feedback-loop resistive heater can stabilize at a set-point temperature within 30 min. The solid lines are sigmoidal fits to the data.
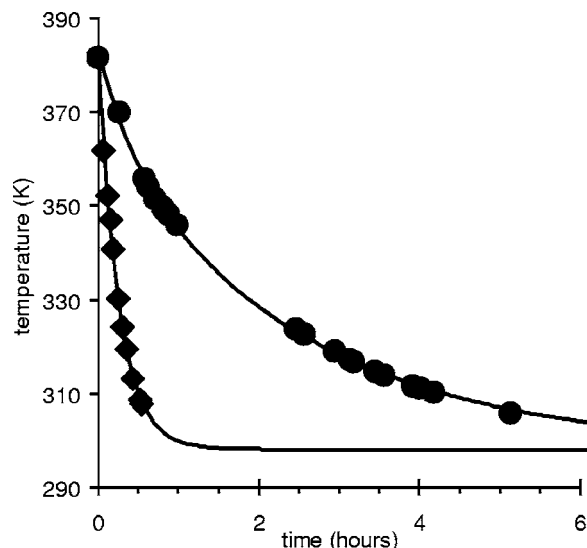

FIG. 3. Temperature performance of the cell without active heating. Under vacuum (●), the cell holds temperature well, decaying with a time constant of 1.9 h. With a constant helium purge (◆), the cell's temperature can be quenched to room temperature within 1 h (time constant 15 min). The solid lines represent an exponential decay fit (for the helium purge data) and a biexponential decay (for the evacuated cell).

organic thin films, the temperature control also allows the sample to be annealed (or undergo other thermal treatment) without being removed from the cell and subsequently re-aligned. This persistence of sample positioning before and after thermal treatment removes some ambiguity in comparing neutron reflectivity curves. It also enables a sequence of experiments to be initiated remotely, or even be completely automated. As can be seen in Fig. 2, the cell can be ramped up above room temperature smoothly, in a short amount of time, and without significant overshoot of the target temperature. The temperature rise is well described by a simple sigmoid with a time constant of 3.7 min. Thus the cell can be considered to have reached a stable temperature within 30 min of a set-point adjustment. Given that typical neutron reflectivity scans take 8–12 h, this temperature stabilization time is not a major concern. However, additional time may need to be given for any sample response to complete. At a given set point, temperature stability is excellent. Deviations from the set point were, at most, 0.02 K (less than 0.01%). This temperature stability is due to the feedback temperature monitoring, but also due to the thermal isolation of the heated sample stage. By evacuating the sample chamber, this thermal isolation can be further enhanced. The cell is able to heat samples to over 200 K above room temperature. For organic thin films, this is typically sufficient to undergo any phase transition of interest. In fact, it is sufficient to degrade most organic materials. The cell can be filled with an inert gas, or entirely evacuated, which helps prevent sample oxidation during thermal treatment.

Figure 3 shows the decrease of the sample environment back to room temperature, where the resistive heater is no longer active. We measured the temperature decay both with an evacuated sample cell and with a constant helium purge at 1 bar. This purge exits directly onto the sample/heater block and serves to efficiently draw off heat from the warm block. In the case of a vacuum environment, the sample temperature decreases slowly, with a time constant on the order of

1.9 h. This demonstrates the excellent thermal isolation of the sample from the laboratory environment. Even without active temperature control, the sample is maintained at high temperature for a significant period of time. With a steady helium stream, heat is drawn off much more efficiently, and in this case the time constant is ~15 min. By changing the pressure of the purge gas, the cooling rate can be varied across a wide range.

The transmission characteristics of the 6 mm thick PMMA window were measured. The material is transparent across the visible (~8% absorption and reflection losses) and induces no polarization change in the incident beam. For more precise optical experiments, the internal volume of the sample cell is sufficient to accommodate the placement of optical components inside the housing, after any perturbing effect of the window material. In fact, a series of optical elements could be constructed as a single unit that replaces the window. This versatile design allows any number of optical experiments to be performed.

RESULTS

The described sample cell was used to study a photoactive polymer thin film. Specifically, thin spin-cast films of an azobenzene polymer, poly(disperse red 1A) (pDR1A), were studied via neutron reflectivity, in order to characterize the photodeformation behavior of this system. The azobenzene chromophore in pDR1A interconverts between *trans*- and *cis*-geometric isomers when irradiated with light near its absorption maximum of 467 nm.[7] This efficient and reversible photochemical isomerization reaction leads to modulation of other material properties. For instance, polarized irradiation can be used to photo-orient the azochromophores.[8] The free surface of an azofilm also undergoes spontaneous mass transport when irradiated with a light intensity or polarization gradient.[9] Macroscopically, thin films have been deformed
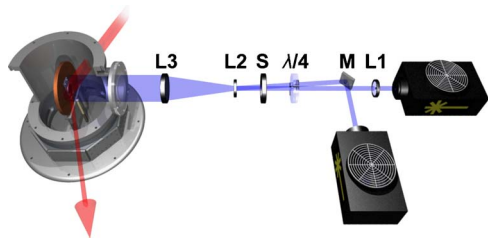
FIG. 4. (Color online) Schematic of neutron reflectometry experiment with simultaneous laser irradiation. Two air-cooled Ar$^+$ lasers (on the right) are used as illumination source. One laser output is adjusted with a converging lens (L1) in order to account for slight differences in laser divergence. A beam from a second laser is reflected off of a mirror (M), making it nearly collinear with the first beam, and passing through a concerted optical train (the angular difference in the two beams has been exaggerated in the diagram, for clarity). The combined beam is converted from linearly polarized to circularly polarized using a wave plate ($\lambda/4$). Diverging (L2) and converging (L3) lenses are then used to expand and collimate the beam, so that they overilluminate the sample with a uniform light intensity. The beam can be turned on and off via computer control of a shutter (S). On the far left, the sample can be seen attached to the copper heating plate, all enclosed in a sealed cell with a transparent window for laser illumination. The neutron beam passes through the sample housing, reflects off of the sample, and travels into a detector.
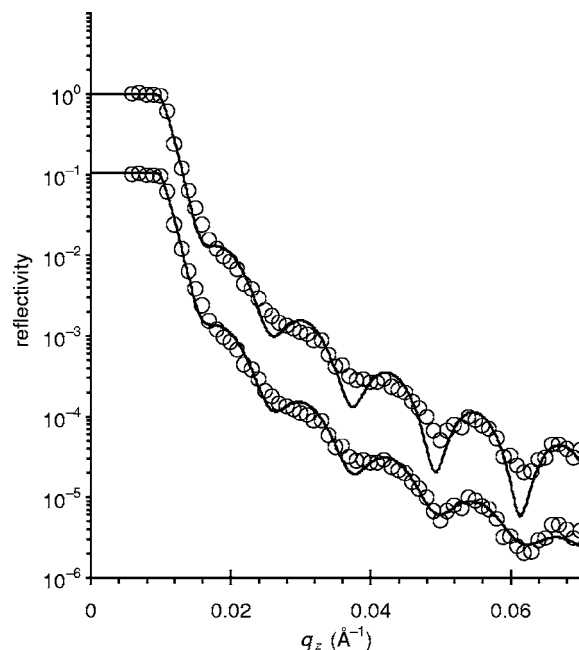

FIG. 5. Comparison of fits used to analyze the neutron reflectivity curves. The data are the same in both cases (a thin azofilm before illumination), but have been offset vertically for clarity. The upper fit is a simple one-box model, which correctly describes the film thickness and density. The lower fit is a more elaborate model that includes a Gaussian distribution of film thickness values. This type of modeling correctly fits both the absolute intensity of the curve, as well as the depth of the minima.

using polarized irradiation.[10] Most recently, the photoexpansion of thin films of azopolymer has been probed via optical techniques.[11] This photoexpansion behavior was studied with neutron reflectometry using the present sample cell. In this setup (Fig. 4), the azosample (spin cast onto a silicon wafer) is placed inside the evacuated sample cell, with the free surface facing the window port. This allows optical irradiation of the azosample at any time, even simultaneous with neutron reflectivity measurements. Furthermore, the cell design allows irradiation under inert atmospheric conditions, and at any temperature. Outside the sample cell, a laser and an optical setup are used to irradiate the thin film. Two ~150 mW argon-ion lasers, emitting at 488 nm, were used as light sources. The combination of two lasers was used to increase irradiation power. Additionally, since the two lasers have no coherence relationship to one another, the dual illumination serves to average out any confounding coherence or interference effects, which are known to lead to mass transport phenomena in azopolymer systems. A mirror is used to direct the two beams nearly collinearly towards a 488 nm $\lambda/4$ plate, which has been adjusted so as to convert the linearly polarized laser beams into a circularly polarized irradiation beam. This circular polarization assures that no in-plane anisotropy is induced in the azomaterial (ratio of intensity along the major and minor axes of 1:1.02 was achieved). A shutter allows for computer-controlled activation of the laser as required by experiment design. Finally, a lens system is used to expand the beam to a sufficient size that it illuminates the entire sample surface uniformly. The PMMA window attenuates the 488 nm probe beam by approximately 8%. The collimated beam was measured to fully irradiate the 24 mm diam sample surface with a uniform intensity of 35 mW/cm^2.

The small sample size is important for studies using optical illumination. A preliminary experiment using a 100 mm silicon wafer gave confounding results. In that experiment, the neutron beam was collimated so as to define a rectangle 77 mm wide by 39 mm tall, on the sample surface. However, over this large area the expanded laser beam was not sufficiently uniform. Thus, some areas of the probed sample saw higher laser intensity than others. The end result was a reflectivity curve that contained contributions from different extents of expansion/contraction. In such a case it is difficult to determine what photophysical effects are occurring, since the neutron beam probes an incoherent sum of different film regions. By using a smaller sample, and overilluminating it with the neutron beam, one achieves a better film uniformity over the probed region. Moreover, the smaller sample size makes it possible to irradiate uniformly with laser light. This makes data interpretation obviously more robust.

The azomaterial was irradiated with laser light for progressively longer periods of time. Typical neutron reflectivity curves, shown in Figs. 5 and 6, show the characteristic fringes due to the thickness and density of the sample. Such curves can be iteratively fit using a variety of models and using the algorithm developed by Parratt.[12] In this case, the PARRATT32 (HMI) software was used, in addition to modified versions of neutron reflectivity calculation source code provided by Thad Harroun (Brock University, Department of Physics). A one-box model produces fringe spacing and positions consistent with the experimental data. However, the amplitude of the fringes (specifically the depth of the minima) is not well described by a one-box model. A more elaborate model, which allows for a small distribution of thickness across the sample surface probed by the neutron beam, correctly reproduces the data (see comparison in Fig. 5). For the samples presented in this article, a Gaussian thickness distribution of 4.5% (~25 Å) was found to be con-
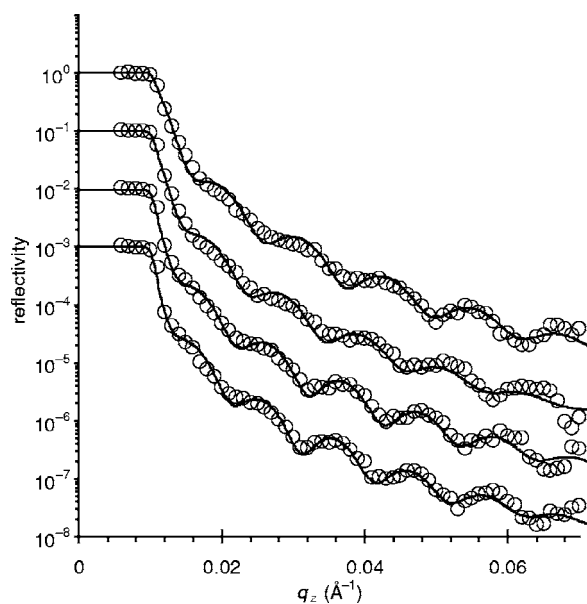
FIG. 6. Neutron reflectivity curves for an azofilm after various amounts of laser illumination. From top to bottom, the curves (offset vertically for clarity) correspond to before irradiation, after 0.4 h total irradiation, after 2.5 h irradiation, and after 7.9 h irradiation. The solid lines are the corresponding distribution-of-thickness fits. The shift of the fringes indicates that the film photoexpands with increased laser exposure.
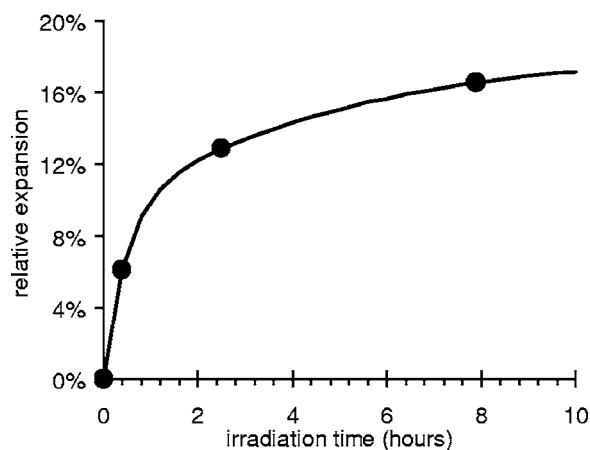

FIG. 7. Relative expansion of an azopolymer film as a function of total laser irradiation time, measured using neutron reflectometry. The data were fit with a biexponential rise-to-max.

sistent with the data. It should be emphasized that this distribution of thickness is not equivalent to a small-scale sample roughness (which would be modeled with a one-box interfacial distribution, and would lead to substantial decrease in the absolute reflectivity for all q_z values); it is, in fact, that different parts of the sample have slightly different thickness, on a size scale larger than the neutron coherence length (this is modeled with an incoherent sum of reflectivity profiles, which causes the minima to be attenuated, without decreasing the absolute reflectivity of the curve). Whether a one-box or a Gaussian distribution of thickness values is used, identical conclusions are obtained.

After irradiation, there is a distinct shift of the fringes (Fig. 6), which indicates that the film has undergone irreversible photoexpansion. With additional irradiation, the film undergoes further expansion. The net expansion with total irradiation time is shown in Fig. 7. The observed effect is indeed material expansion, as the sample's scattering length density decreased with corresponding expansion (that is, the area under the film profile curve is constant, to within $\sim 2\%$). The sample cell used, however, allows us to additionally probe the sample during illumination. A typical neutron reflectivity curve requires 8–12 h of data collection, which is far too long to capture the dynamics of the azobenzene photoexpansion. However, one can measure a small portion of the reflectivity curve in order to characterize the behavior over time. We probed the change in neutron reflectivity at specific q_z values, during irradiation with laser light (Fig. 8). In Fig. 8(a), one can see the change in reflectivity at $q_z=0.02$ Å^{-1}, and in (b), the reflectivity at $q_z=0.05$ Å^{-1}. The reflectivity at $q_z=0.05$ Å^{-1} changes in an oscillatory and complex way as laser irradiation proceeds. This is due to the fact that the Kiessig fringes, which are shifting as the film photoexpands,

pass in and out of the observation window. By comparison, the monotonic behavior at $q_z=0.02$ Å^{-1} closely relates to the observed change in thickness. This is because near the critical reflectivity edge, a single fringe is being shifted towards lower q_z. Furthermore, scanning at small q_z is considerably faster than scanning at high q_z, because the much higher absolute reflectivity requires shorter integration times to achieve reasonable statistics. Clearly some regions of the reflectivity curve are more valuable than others for interpreting the kinetics and dynamics of systems. With appropriate choice of q_z, one is able to follow, in real time, any material
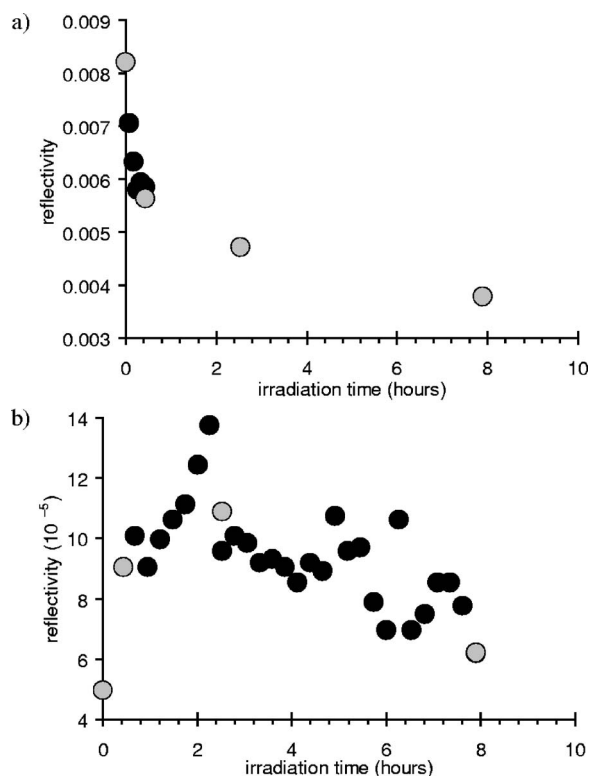

FIG. 8. Neutron reflectivity signals at $q_z=0.02$ Å^{-1} (a) and $q_z=0.05$ Å^{-1} (b). The black symbols refer to measurements during laser illumination, whereas the gray symbols refer to measurements in between successive laser irradiation steps. The monotonic data for smaller q_z provide a more meaningful measure of photophysical change than do the data at larger q_z.
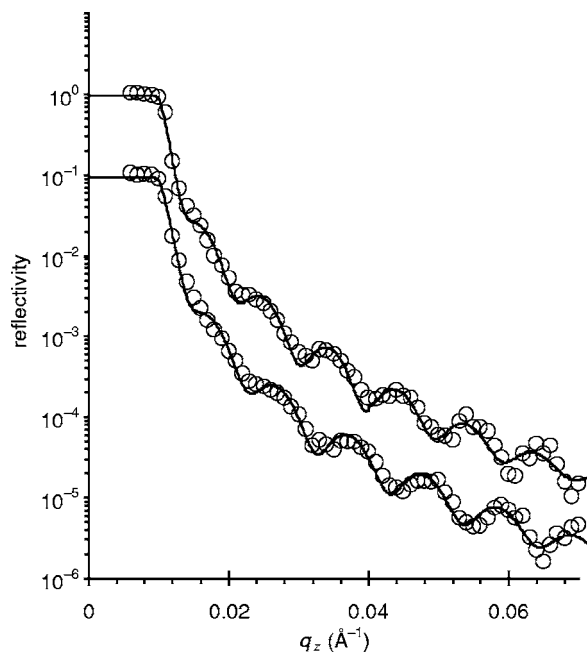
FIG. 9. Neutron reflectivity curves measured at different temperatures (offset vertically for clarity). The upper curve is a thin film, at room temperature, that has been laser irradiated. The lower curve is the same film, heated to, and maintained at 353 K. The distribution-of-thickness fits to the data (solid lines) show that the photoexpanded film thermally contracts.

changes. This serves two purposes: one, it is possible to determine when a system has reached a stable state and can then be subjected to a full reflectivity scan (i.e., the sample will not be changing during the measurement); two, it is possible to determine the kinetic behavior of material transformations.

Consistent with previous optical investigation of these materials,[11] there is a substantial irreversible photoexpansion and a secondary elastic expansion of the material that occurs only when the illuminating light is on. This explains the slight difference between the reflectivity intensity when the laser is on versus off. Such changes would not be possible to measure if the sample needed to be removed from the neutron beam for light irradiation. In addition to monitoring material changes during light illumination, the present cell en-

ables measurements during temperature ramping, or while maintaining the sample at a given temperature. Figure 9 shows an example of a photoexpanded sample that was subsequently treated thermally, which led to contraction of the material. All of these scans were taken without removing the sample from the cell, which makes alignment much faster, and removes any ambiguity that would arise from inconsistent sample placement. The control of the sample atmosphere enabled it to be annealed through its glass transition temperature without any danger of oxidation or other material damage. By controlling environmental parameters, this cell thus offers the possibility of much higher experimental reproducibility.

DISCUSSION

We have designed, built, and tested a unique neutron reflectometry sample cell, which is able to maintain a sample at a desired temperature under controlled atmospheric conditions, and further allows for simultaneous irradiation or probing with light. The ability to measure neutron reflectivity during illumination and/or temperature adjustments generates new possibilities for experimental studies. This cell is also versatile, accommodating a range of possible optical components, and could even be used with other neutron scattering techniques.

[1] H. Kiessig, Ann. Phys. **10**, 769 (1931).
[2] T. P. Russell, Mater. Sci. Rep. **5**, 171 (1990).
[3] L. Eldada, Rev. Sci. Instrum. **75**, 575 (2004); C. López, Adv. Mater. (Weinheim, Ger.) **15**, 1679 (2003).
[4] K. Ichimura, Chem. Rev. (Washington, D.C.) **100**, 1847 (2000).
[5] C. Kempe, M. Rutloh, and J. Stumpe, J. Phys.: Condens. Matter **15**, S813 (2003).
[6] T. A. Harroun, H. Fritzsche, M. J. Watson, K. G. Yager, O. M. Tanchak, C. J. Barrett, and J. Katsaras, Rev. Sci. Instrum. **76**, 065101 (2005).
[7] H. Rau, in *Photochemistry and Photophysics*, edited by J. Rebek (CRC, Boca Raton, FL, 1990), Vol. 2, pp. 119–141.
[8] A. Natansohn and P. Rochon, Chem. Rev. (Washington, D.C.) **102**, 4139 (2002).
[9] K. G. Yager and C. J. Barrett, Curr. Opin. Solid State Mater. Sci. **5**, 487 (2001).
[10] Y. Yu, M. Nakano, and T. Ikeda, Nature (London) **425**, 145 (2003); T. Ikeda, M. Nakano, Y. Yu, O. Tsutsumi, and A. Kanazawa, Adv. Mater. (Weinheim, Ger.) **15**, 201 (2003).
[11] O. M. Tanchak and C. J. Barrett, Macromolecules **38**, 10566 (2005).
[12] L. G. Parratt, Phys. Rev. **95**, 359 (1954).